

thermotropic differences seem to correlate with important differences in the behaviour of the studied preparations once subjected to interfacial compression-expansion cycling, specially with respect to the stability of repeatedly compressed films.

Local Calcium Signaling

1226-Pos Probing Nanodomain Ca^{2+} of Ca^{2+} Channels using a Genetically Encoded Ca^{2+} Sensor (TN-XL) Fused to N-type Channels

Lai Hock Tay¹, Michael R. Tadross¹, Ivy E. Dick¹, Wanjun Yang¹, Marco Mank², Oliver Griesbeck³, David T. Yue¹

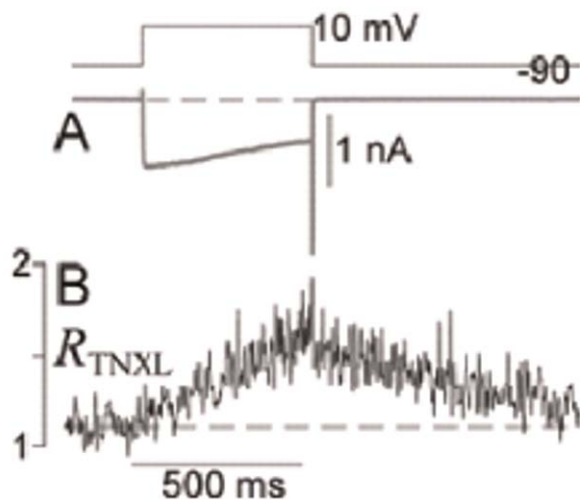
¹ Johns Hopkins University, Baltimore, MD, USA

² Max Plank Institute for Neurobiology, Martinsried, Grenada

³ Max Plank Institute for Neurobiology, Martinsried, Germany.

Board B202

Numerous processes sense Ca^{2+} within nanometers of the cytoplasmic mouth of Ca^{2+} channels. Unfortunately, direct resolution of this 'nanodomain' Ca^{2+} has been lacking, except for a recent study wherein chemical fluorescent Ca^{2+} indicators were selectively reacted with $\text{Ca}_v1.2$ channels (Tour *et al*, *Nature Chem Biol* 3:423). A limitation, however, was the exceedingly low open probability P_O of these channels. Here, we undertake a different approach, fusing a genetically encoded Ca^{2+} indicator (GECI) to N-type ($\text{Ca}_v2.2$) channels. Channels are joined to TN-XL, a CFP/YFP-FRET-based GECI built around the Ca^{2+} sensing protein troponin C (Mank *et al*, *Biophys J*, 90:1790); and $\text{Ca}_v2.2$ TN-XL fusions maintain a high $P_O \sim 0.6$. Using TIRF imaging to enrich for GECI signals from the surface membrane, we resolve nanodomain Ca^{2+} signals, as isolated with 10 mM internal EGTA. The figure displays the whole-cell Ca^{2+} current of $\text{Ca}_v2.2$ TN-XL (A), along with the corresponding GECI Ca^{2+} readout (B, R_{TNXL}), averaged over several cells. We modeled the kinetically slowed TN-XL response (Tay *et al*, *Biophys J*, in press), and this analysis accords with underlying Ca^{2+} transients reaching $\sim 25\text{--}50 \mu\text{M}$, as predicted by prior theory.



1227-Pos Familial Hemiplegic Migraine FHM2 Mutations Disrupt Local and Global Calcium Signaling

Ian F. Smith¹, Shaochun Ma¹, Neil Beri¹, Cindy Shih¹, Rhoda Blostein², Ian Parker¹, J. Jay Gargus¹

¹ Univ California, Irvine, Irvine, CA, USA

² McGill, Montreal, QC, Canada.

Board B203

FHM2 is an autosomal dominant, classical migraine subtype associated with missense mutations in the $\alpha 2$ isoform of the Na, K-ATPase. This isoform of the Na, K-ATPase plays a role in Ca^{++} homeostasis, and spatiotemporal properties of Ca^{++} release regulate processes as diverse as differentiation, synaptic plasticity and apoptosis.

We hypothesize that perturbations in Ca^{++} homeostasis may be a proximal signaling defect in FHM2. We thus investigated whether FHM2 mutants disrupt Ca^{++} signaling in stable transformant human neuronal SH-SY5Y cells expressing either wild-type $\alpha 2$ or the T345A or R689Q FHM2 mutations of $\alpha 2$. Ca^{++} signals evoked by $100 \mu\text{M}$ carbachol were reduced in both mutants, and Ca^{++} oscillations were suppressed. Local IP3 Ca^{++} signals were evoked using UV-flash photolysis of caged IP3 in cells loaded with EGTA so as to 'balkanize' Ca^{++} waves into discrete localized Ca^{++} puffs. Ca^{++} puffs evoked in FHM2 mutant transformants occurred with a similar frequency, yet lower amplitudes than in wild-type transformant cells. Imaging by total internal reflection microscopy revealed that the majority of puff sites are located adjacent to the plasma membrane, and these membrane-associated puffs also showed significantly reduced amplitudes in cells expressing either mutant. These FHM2 mutant effects could all be observed even without inhibiting the normal endogenous human sodium pumps, simulating the heterozygous disease state. Given that the T345A and R689Q mutations affect Na, K-ATPase enzyme kinetics and pump function in different ways and yet lead to similar disruptions in Ca^{++} signaling we hypothesize that alterations in Ca^{++} signaling may be the primary shared pathogenic mechanism common to FHM2 mutations, and may explain the similarity of that disease to FHM1, caused by dominant P/Q calcium channel mutations.

Supported by grants NIH GM 40871 (I.P.) and NIH MH 71433 (J. J.G.)

1228-Pos Astrocyte Intracellular Calcium Dynamics Measured With Total Internal Reflection Fluorescence Microscopy

Eiji Shigetomi, Baljit S. Khakh

Department of Physiology, David Geffen School of Medicine, UCLA, Los Angeles, CA, USA.

Board B204

Intracellular Ca^{2+} levels in astrocytes are set by Ca^{2+} entry through channels and transporters on the plasma membrane, in addition to

Ca^{2+} release from intracellular stores. Increases in intracellular Ca^{2+} can lead to Ca^{2+} -dependent gliotransmitter release, and the amount of Ca^{2+} level at the plasma membrane may be an important factor for this process. Unlike neurotransmitter release, most of the Ca^{2+} involved in gliotransmitter release is thought to arrive at the plasma membrane from intracellular stores. To analyze Ca^{2+} dynamics at the plasma membrane, we loaded fluo4-AM into rat hippocampal astrocytes (co-cultured with neurons) and measure Ca^{2+} within ~ 100 nm of the plasma membrane using total internal reflection fluorescence microscopy (TIRF); we simultaneously measured global intracellular Ca^{2+} using epifluorescence microscopy (EPI). We found about 63% of spontaneous Ca^{2+} transients observed in EPI were correlated with those in TIRF. However, about 37% of transients observed in EPI were not observed in TIRF. Both types of transients were observed in the presence of TTX, suggesting that they are independent of local neuronal activity. In conditions where large amounts of Ca^{2+} was released from intracellular stores using saturating concentrations of G-protein coupled receptor (GPCR) agonists, almost all global Ca^{2+} changes also elevated Ca^{2+} near the plasma membrane, but the kinetics between TIRF and EPI varied with the specific GPCR activated. Overall, our data suggest that not all spontaneous Ca^{2+} transients measured globally within astrocytes elevate Ca^{2+} significantly near the plasma membrane, and that activation of GPCRs on astrocytes does not necessarily result in physiological Ca^{2+} transients in astrocytes. The relevance of these data to astrocyte physiology and gliotransmitter release will be presented.

1229-Pos Imaging Synaptic Calcium Signalling In Cochlear Hair Cells

Thomas Frank¹, Andreas Neef², Tobias Moser^{1,3}

¹Medical School, University of Goettingen, Goettingen, Germany

²Max-Planck Institute for Dynamics and Self-organization, Goettingen, Germany

³CMPB, Goettingen, Germany.

Board B205

One important function of calcium in the inner hair cell (IHC) is the triggering of neurotransmitter release. Strong evidence indicates that clusters of calcium channels ($\text{Ca}_v1.3$ type) at the active zones of inner hair cells mediate the calcium influx at this ribbon synapse (Brandt et al., 2005). Hence, calcium signalling is expected to be confined to discrete regions. Yet, a diffuse and homogenous increase in intracellular calcium in the basal half of mouse IHCs has been reported (Kennedy and Meech, 2002). Using a low-affinity Ca^{2+} indicator, and excess of EGTA, we visualize distinct calcium entry sites by confocal microscopy.

We characterized size, kinetics, and voltage-dependence of these calcium signals. In most cases, 2 mM $[\text{EGTA}]_{\text{in}}$ inhibited spatial spread of the F_{Ca} signal. Under these conditions, the width of the calcium signal was found to lie in the range of 0.7 to 1.0 μm . Furthermore, kinetic measurements of the F_{Ca} signals were obtained in the spot-detection mode of a confocal microscope with high temporal resolution. The majority of F_{Ca} signals showed a rapid rise component, with time-constants ranging from < 1 to 5 ms - in the presence of intracellular Cs^+ . In addition, many transients exhibited a slower rise component (range: 10 to > 100 ms). The decline of the

F_{Ca} signal was likewise found to be bi-exponential in most of the cases ($\tau_{\text{fast}} = 1$ to < 10 ms; $\tau_{\text{slow}} = 10$ to < 100 ms). The F_{Ca} signals exhibited similar voltage-dependence as the $\text{Ca}_v1.3$ -mediated whole-cell current. We are currently working on a characterization of these calcium signals in the presence of endogenous buffers. Our results refine the view of presynaptic calcium signalling in the mouse IHC, and may aid better understanding of the channel distribution in these cells.

1230-Pos Analysis of Localized Ca^{2+} Alterations During Cell Death from Noisy Data

Man-Soo B. Hong

University of Virginia, Landover Hills, MD, USA.

Board B206

Fluctuations in intracellular calcium ion (Ca^{2+}_i) levels are believed to participate in a myriad of physiological and pathological intracellular events. In an attempt to investigate localized alterations in Ca^{2+}_i dynamics in a cell-based neurodegeneration model, we used Fura-2/AM dye to monitor Ca^{2+}_i ion levels in the human SH-SY5Y neuroblastoma cells induced to undergo apoptosis with 500 nM staurosporine (STS) over a 24 h period. Using rapid illumination frequency at 5 Hz per 340/380 nm excitation wavelength pair, streaming image acquisition and analysis of 12 very small regions of interest (ROI) of $\sim 86.5 \mu\text{m}^2$ in either peri-nuclear (PN) or distal (DST) cytoplasmic locations, we captured micro-regional signals ("Ca2+i ripples") at selected eight time points that were then processed either linearly or nonlinearly into dominant frequencies and peak amplitudes. STS exposure induced caspase-dependent apoptosis that was blocked by Ca^{2+}_i chelation with BAPTA/AM. In some SH-SY5Y cells undergoing apoptosis, submaximal 10 μM treatment with the inositol 1,4,5-trisphosphate (IP3)-agonist carbachol (CCh) produced several-fold increases in power spectral densities and peak amplitudes of the Ca^{2+}_i ripples in both PN and DST regions with a trend towards increased magnitude with greater time of STS exposure. These STS-induced changes were blocked by zVAD.fmk, implicating one or more caspases. Our findings seemed to indicate that buried within typical Ca^{2+}_i waves are rhythmic fluctuations in local regional Ca^{2+}_i levels that are modulated by an IP3 stimulus to yield increased peak spectral power and peak amplitude. These appeared to become dysregulated and amplified during caspase-mediated apoptosis and may contribute to the Ca^{2+}_i -dependency of STS-induced apoptosis. A more thorough study of this phenomenon may yield insight into the heterogeneity of small regional Ca^{2+}_i signaling and its alteration during cell death.

1231-Pos Spatially Restricted Ca^{2+} Transients Reflect Release By The SR In Rabbit Ventricular Myocytes

Mark R. Fowler, Godfrey L. Smith

University of Glasgow, Glasgow, United Kingdom.

Board B207

Global release of intracellular Ca^{2+} is the spatial and temporal summation of elementary Ca^{2+} release events. Some whole-cell electrophysiological protocols often use high concentrations of Ca^{2+} chelator that buffers Ca^{2+} to physiological levels whilst spatially restricting the movement of intracellular Ca^{2+} . We examined the hypothesis that Ca^{2+} transients were present with high Ca^{2+} buffering, based on the assumption that Ca^{2+} chelators bind Ca^{2+} with definite length constants. Rabbit ventricular myocytes were whole-cell patch clamped using Cs- and TEA-rich internal and external solutions (1.8mM Ca^{2+}) with 50mM EGTA (170nM free Ca^{2+}) in the patch pipette. Ca^{2+} was monitored using Fura-2 (100 μM , pentapotassium salt). Cells were depolarized from a holding potential of -80mV to 0mV for 300ms at 0.5Hz. 50mM EGTA restricts the movement of intracellular Ca^{2+} to approx. 48nm. This did not significantly effect τ_{fast} of $I_{\text{Ca,L}}$ inactivation ($8.8 \pm 0.9\text{ms}$, $n=14$), compared to 0.3mM EGTA ($9.4 \pm 0.5\text{ms}$, $n=6$) and 1mM EGTA ($8.9 \pm 0.3\text{ms}$, $n=9$), suggesting retention of localized signaling. Under these conditions, averaging intracellular Ca^{2+} revealed small, transient, elevations in intracellular Ca^{2+} . The time to peak of the transient was $16.3 \pm 1.3\text{ms}$, ($n=19$). SR inhibition with thapsigargin (25 μM) significantly prolonged the time to peak of the Ca^{2+} transient ($29.5 \pm 3\text{ms}$, $n=8$, $P<0.05$). Ca^{2+} transient amplitude was significantly decreased, but not abolished, following SR inhibition, which also significantly prolonged τ_{fast} of $I_{\text{Ca,L}}$ ($8.8 \pm 0.9\text{ms}$, $n=14$ vs. 23.4 ± 0.9 , $n=23$, $P<0.05$). These data describe localized Ca^{2+} signals, recorded with Fura-2, that occur in a spatially restricted region of ~50nm. The amplitude and time course of this signal is sensitive to SR inhibition and is important for regulation of $I_{\text{Ca,L}}$.

1232-Pos A Mechanistic Model of Ca^{2+} /Calmodulin Dependent Kinase II Interactions with L-type Ca^{2+} Channels in the Cardiac Myocyte

Yasmin L. Hashambhoy, Joseph L. Greenstein, Raimond L. Winslow

Johns Hopkins University, Baltimore, MD, USA.

Board B208

Many reports indicate that Ca^{2+} /calmodulin-dependent protein kinase II (CaMKII) may play an important role in L-type Ca^{2+} channel (LCC) facilitation, and abnormal increases in CaMKII activity have been shown to have pro-arrhythmic consequences. Facilitation may arise from the combination of multiple mechanisms, such as increased rate of recovery from Ca^{2+} -dependent inactivation (CDI) and a shift in modal distribution from mode 1, the dominant mode of LCC gating, to mode 2, in which openings are prolonged. However, it is difficult to experimentally dissect the distinct mechanisms of CaMKII-mediated modulation of LCC facilitation as both are triggered by similar events. Changes in modal distribution or CDI will feedback on each other, and both phenomena result in increased LCC current. In order to elucidate how CaMKII directly influences LCC facilitation, we have developed a deterministic state model that describes CaMKII activity as a

function of local concentrations of Ca^{2+} , buffers and phosphatases, and explicitly characterizes CaMKII mechanisms of action on LCCs. The model is developed based on data from CaMKII-LCC single channel studies, such as altered open probability and shifts in modal gating distribution in the presence of constitutively active CaMKII or mutant channels. We are able to quantify the relative contributions of recovery of CDI and shifts in modal gating distribution on LCC facilitation. Integration of the CaMKII model into a computational model of the canine ventricular myocyte provides the means to better understand how CaMKII activity is influenced by factors such as kinase localization, heart rate, and the level of phosphatase activity. In addition, the model elucidates the role of CaMKII activity on LCC current amplitude and kinetics, AP shape and duration, and the appearance of pro-arrhythmic events such as early afterdepolarizations.

1233-Pos Role Of Acetylcholine Activated Potassium Current ($I_{\text{K}_{\text{Ach}}}$), Hyperpolarization Activated Current (I_{f}), Protein Kinase A (PKA)-Dependent Phosphorylation And Ca^{2+} Cycling In Muscarinic Receptor (M_2R) Regulation Of Spontaneous Action Potential Rate (APR) In Isolated Rabbit Sinoatrial Node Cells (SANC)

Alexey E. Lyashkov, Tatiana M. Vinogradova, Antoine Younes, Yue Li, Bradley Nuss, Harold A. Spurgeon, Edward G. Lakatta

NIH/NIA, Baltimore, MD, USA.

Board B209

Multiple potential mechanisms can link M_2R activation of SANC to a reduction in APR via contribution of $I_{\text{K}_{\text{Ach}}}$, I_{f} or $I_{\text{Ca,L}}$ currents and the PKA modulated sarcoplasmic reticulum (SR) Ca^{2+} signaling. The M_2R agonist Carbachol (CCh) 10nM to 1 μM reduced APR by 8% to 100%, respectively, (50% of maximal reduction at 0.1 μM ; average APR 182 ± 11.1 beat/min, $n=56$). This effect of CCh was completely blocked by PTX, confirming a G_i protein involvement. Maximum Diastolic Potential (MDP) hyperpolarization, a marker of $I_{\text{K}_{\text{Ach}}}$ current contribution to the CCh effect during spontaneous beating, increased up to 8.9% with increasing [CCh]; average MDP in control -60.15 ± 1.3 mV ($n=56$). Terteapin Q (TQ, 1 μM), a highly potent peptide blocker of $I_{\text{K}_{\text{Ach}}}$, blocked $I_{\text{K}_{\text{Ach}}}$ current and also MDP hyperpolarization induced by CCh, but only partially blocked the CCh reduction of APR ($6 \pm 1.1\%$ at 10nM to $29 \pm 6.5\%$ at 1 μM CCh, $n=26$). CsCl (2mM) completely blocked I_{f} current (under voltage clamp), but failed to reduce APR at any [CCh], either in the presence or absence of TQ. CCh at 0.1 μM or 1 μM , in the presence of 100 μM IBMX, reduced SANC cAMP by $21 \pm 9\%$ and $34 \pm 13\%$, respectively ($n=5$), and reduced PKA-dependent phospholamban phosphorylation by $42 \pm 1\%$ and $32 \pm 1.9\%$. CCh (0.1 μM) exposure for 3 min reduced the frequency, amplitude and size by 17%, 21.7% and 18.2% of local subsarcolemmal Ca^{2+} releases detected by

confocal imaging concurrently with a 52% reduction in APR. We conclude that half maximal effectiveness of CCh accounts for $55 \pm 4.5\%$ of Gi dependent APR reduction; $30 \pm 6\%$ is attributable to cAMP-PKA-SR Ca^{2+} cycling (SR Ca^{2+} clock) and 25% to IK_{ACH} activation (membrane clock).

1234-Pos Calcium Blinks In Rabbit And Rodents: SR Calcium Depletion Signals Reveal New Features In Subcellular Calcium Signaling

Didier X.P. Brochet^{1,2}, Dongmei Yang², W. Jonathan Lederer¹, Heping Cheng^{3,2}

¹ University of Maryland Biotechnology Institute, Baltimore, MD, USA

² National Institute on Aging, NIH, Baltimore, MD, USA

³ Peking University, Beijing, China.

Board B210

Elementary calcium release events (Ca^{2+} sparks) underlie excitation-contraction coupling in heart and have been visualized in diverse tissues (muscles, neurons and even non-excitable cells) and species (rat, mouse, rabbit, dog, cat and human). As Ca^{2+} efflux from the sarcoplasmic reticulum (SR) produces the cytosolic Ca^{2+} spark, local depletion of Ca^{2+} (Ca^{2+} blink) is developing within the SR. The depletion signal provides a rapid (millisecond) signal with high spatial resolution (100 nm), revealing the inner workings of the intracellular Ca^{2+} storage organelles (Brochet *et al.*, PNAS, 2005). While Ca^{2+} blinks were initially described in rabbit ventricular myocytes, we have examined myocytes from small rodents (mouse and rat), and determined that they robustly reveal the dynamics of SR lumenal Ca^{2+} .

The size (full width at half maximum) of Ca^{2+} blinks in rabbit, rat and mouse was not statistically different. In contrast, the recovery time (τ) of blinks was slower in rodents (67.6 and 66.6 msec in rat and mouse, respectively) than in rabbit (50.2 msec). The blink amplitude ($\Delta F/F_0$) was greater in rabbit (0.218) than in rat and mouse (0.09 and 0.10, respectively) and the density of dyads was about 50% higher in rodent compare to rabbit (unpublished observations from A. DiMaio and C. Franzini-Armstrong). Taken together, these results show important differences in animals with established differences in Ca^{2+} signaling behavior. It suggests that these tools may also reveal key new features in disease (e.g. arrhythmogenesis) where abnormal Ca^{2+} dynamics are suspected of contributing to the primary pathology.

263 Must be less than 300 words.

1235-Pos Low Amplitude of Late Ca^{2+} Spikes is a Result of Decreased Calcium Release Flux

Alexandra Zahradnikova Jr., Eva Polakova, Jana Pavelkova, Ivan Zahradnik, Alexandra Zahradnikova

Institute of Molecular Physiology and Genetics, Bratislava, Slovakia.

Board B211

The extent and synchrony of calcium release from individual calcium release sites in cardiac myocytes varies considerably. Our aim was to compare latencies and amplitudes of local calcium release events to reveal possible common determinants.

Local calcium release events (Ca-spikes) were evoked by calcium currents in voltage-clamped isolated rat ventricular myocytes. The cells were excited by a step depolarization from -50 to 0 mV. Ca-spikes were measured using 0.1 mM fluo-3 as the calcium indicator and 1 mM EGTA to limit calcium diffusion, and compared with simulated Ca-spikes [1]. Three-dimensional convolution of calcium-bound fluo-3 concentration with a Gaussian kernel was used for simulation of Ca-spike images. Both the measured and simulated local calcium release events were analyzed as previously described [1]. The amplitudes as well as kinetic parameters of simulated Ca-spikes were strongly dependent on the distance of the event from the focal plane.

The amplitude-latency relationship of experimental calcium spikes revealed the presence of two, early and late, populations of calcium release events. In early events, the relationships between their fluorescence amplitude and time-to-peak or duration at half amplitude were similar to that of simulated events and consistent with uniform calcium release flux amplitude. In late events, the kinetics were faster than expected if their amplitude was low due to larger distance from the focal plane but were as expected if the calcium release flux was decreased. These results indicate that either some ryanodine receptors are inactivated at these release sites, or calcium contents of their luminal environment is decreased.

Support: APVT-51-031104, EU Contract No. LSHM-CT-2005-018833/EUGeneHeart, NIH-FIRCA-R03-TW-05543.

References

1. Zahradnikova A., jr. *et al.* Kinetics of calcium spikes in rat cardiac myocytes. *J Physiol.* 578: 677–691, 2007.

1236-Pos Dependence of Local Calcium Release Activation on the Distribution of DHPR Calcium Channel Open Times

Eva Polakova, Alexandra Zahradnikova Jr., Jana Pavelkova, Ivan Zahradnik, Alexandra Zahradnikova

Institute of Molecular Physiology and Genetics, Slovak Academy of Sciences, Bratislava, Slovakia.

Board B212

The mechanism of activation of local calcium release by calcium current (I_{Ca}) was investigated in rat cardiac myocytes using patch-clamp and confocal microscopy. Calcium spikes were recorded using the calcium indicator OG-5N. A temporally well defined surge of calcium influx was applied by preactivating calcium channels (DHPRs) above their reversal potential and then stepping to a negative tail potential, at which I_{Ca} rapidly deactivated. The amplitude and duration of calcium influx were modulated by varying prepulse duration or tail potential, and by applying the agonist BayK8644 to prolong DHPR open times. Probability density of the measured calcium spike latency distribution was described using a

model based on exponential distribution of DHPR open times and on higher-order kinetics of ryanodine receptor (RyR) activation accounting for multiple Ca^{2+} -binding sites. The distribution of spike latencies at -120 mV, when reopenings of DHPRs were virtually absent, was in excellent accordance with the theoretical prediction for DHPR open times of ~0.5 ms and activation time constant of RyRs below 1 ms in the absence of BayK8644. Coupling fidelity at -120 mV increased almost twice in the presence of BayK8644 but was still much less than one. The high probability of calcium spike activation could be explained only by the presence of many DHPRs at individual release sites. In the presence of DHPR reopenings, spike probability was increased over the theoretical value. These data suggest that the coupling fidelity of individual DHPR openings is inherently low due to their exponential open time distribution, and that control of excitation-contraction coupling is achieved by modulating the number of DHPR openings occurring in parallel (multiple channel openings) and in series (channel reopenings).

Supported by APVT-51-031104, EU Contract No. LSHM-CT-2005-018833/EUGeneHeart, and NIH-FIRCA-R03-TW-05543.

1237-Pos Sarcoplasmic Reticulum Refilling Via NCX-mediated Ca^{2+} -entry Is Impaired By Mitochondria Fragmentation And Redistribution In Aorta Smooth Muscle Cells

Damon Poburko

University of Geneva, Geneva, Switzerland.

Board B213

The Na^{+} - Ca^{2+} exchanger (NCX) is increasingly recognized as a physiological mediator of agonist-induced Ca^{2+} -entry. NCX-mediated Ca^{2+} entry (NCE) is stimulated by receptor-operated, non-selective cation channels locally elevating $[\text{Na}^{+}]_i$ at junctions of the plasmalemma and sarcoplasmic reticulum (SR). We directly measured $[\text{Ca}^{2+}]_{\text{SR}}$ with the "cameleon" probe D1ER to test the hypothesis that NCE efficiently refills SR Ca^{2+} stores following stimulation of rat aorta smooth muscle cells with ATP, and that perinuclear mitochondria facilitate SR refilling by transferring the incoming Ca^{2+} ions to the SR. ATP transiently reduced $[\text{Ca}^{2+}]_{\text{SR}}$ from ~1mM at rest to 100–200 microM, compared to 20–50µM following SERCA inhibition with cyclopiazonic acid. Removing extracellular Ca^{2+} prevented SR refilling, and NCX inhibition with KB-R7943 (10 microM) delayed refilling by 35±5sec and slowed the subsequent rate of refilling. Mitochondrial NCX inhibition with CGP-37157 (20 microM) slowed and reduced SR refilling without delaying its on-set, whereas F_1F_0 -ATPase inhibition with oligomycin (5 microg/ml) did not affect SR refilling. To disrupt the NCX-mitochondria association, we over-expressed hFis1, a protein that fragments mitochondria and moves them away from the plasmalemma. hFis1 over-expression increased $[\text{Ca}^{2+}]_{\text{cyto}}$ and decreased $[\text{Ca}^{2+}]_{\text{mito}}$ responses to NCX-mediated Ca^{2+} -entry stimulated by ATP or removal of extracellular Na^{+} , indicating impaired mitochondrial NCE buffering. Concomitantly, ATP-mediated SR Ca^{2+} depletion was increased, and the rate and extent of SR refilling impaired. We conclude that NCE and Ca^{2+} -transit through neigh-

boring mitochondria mediates efficient refilling of SR Ca^{2+} stores following purinergic stimulation, and likely precedes the activation of store-operated Ca^{2+} entry. Furthermore, these findings demonstrate that disruption of normal mitochondrial morphology and subcellular distribution impairs the localized transfer of Ca^{2+} influx to the SR, causing impaired refilling of Ca^{2+} stores and potentially deleterious enhancement of $[\text{Ca}^{2+}]_{\text{cyto}}$ responses following agonist stimulation.

1238-Pos Spatial Organization Of RyRs And BK Channels Underlies The Activation Of STOCs By Ca^{2+} Sparks In Mouse Airway Myocytes

Lawrence M. Lifshitz, Jeffrey D. Carmichael, Karl D. Bellve, Richard A. Tuft, Kevin E. Fogarty, Ronghua ZhuGe

UMass Med Sch, Worcester, MA, USA.

Board B214

Opening of ryanodine receptors (RyRs) in sarcoplasmic reticulum generates highly localized, short-lived Ca^{2+} transients, designated as Ca^{2+} sparks. In smooth muscle, these events activate BK channels to generate spontaneous transient outward currents (STOCs), which in turn regulate the contractile state of the cells. However, the spatial organization of RyRs and BK channels underlying the functional coupling between Ca^{2+} sparks and STOCs is not fully understood. We addressed this question in mouse airway myocytes by immunocytochemical localization of three types of RyRs and the alpha subunit of BK channels with 3D imaging, and by measuring STOCs with the whole-cell patch-clamp method and simultaneous imaging of Ca^{2+} sparks with high-speed, widefield digital microscopy. Our immunocytochemical analysis reveals that both BK channels and RyRs form clusters, and only a subset of RyR1 and RyR2 colocalize with or are in proximity to BK channels. Our functional studies indicate that

1. the opening of 10–30 RyRs produces Ca^{2+} sparks, which initiate STOCs by activating approximately 30 clustered BK channels, and
2. BK channels underlying STOCs sense a $[\text{Ca}^{2+}]$ on the order of 10 µM during Ca^{2+} sparks.

Combining these data with computer simulation of Ca^{2+} spark and BK channel kinetics, we propose a mechanistic model of how Ca^{2+} sparks activate STOCs.

(Supported by NIH)

1239-Pos Luminal Regulation of Ca^{2+} Release Creates Apparently Separate Stores on a Single Sarcoplasmic Reticulum Structure in Smooth Muscle

John G. McCarron, Marnie L. Olson

University of Strathclyde, Glasgow, United Kingdom.

Board B215

The sarcoplasmic reticulum (SR) achieves selective activation of processes such as gene expression, growth and metabolism, in part, by being able to compartmentalize functions in various regions of the cell. One explanation, for the compartmentalization of function, is the SR comprises a series of structurally-separate Ca^{2+} storage elements each with various arrangements of the release channels and sensitivities to ligands. This study, in single smooth muscle cells, addresses whether or not the SR exists as multiple, separate, Ca^{2+} stores or as a single lumenally-continuous entity throughout the cell. From one small site on the cell, the entire SR could be depleted via either ryanodine receptors (RyR) or IP_3 receptors (IP_3R). The entire SR could also be refilled from one small site on the cell. The SR is a single lumenally-continuous structure in which Ca^{2+} is in free diffusional equilibrium throughout. Notwithstanding the luminal-continuity, regulation of the opening of RyR and IP_3R , by the $[\text{Ca}^{2+}]$ within the SR, may create several receptor arrangements on apparently separate stores. IP_3R and RyR may appear to exist entirely on a single store, and there may seem to be additional SR elements which express either only RyR or only IP_3R . The various SR receptor arrangements and apparently separate Ca^{2+} storage elements exist in a single lumenally-continuous SR structure.

Supported by the Wellcome Trust and British Heart Foundation

1240-Pos Simultaneous Imaging of Subplasma Membrane and Bulk Cytoplasmic Average Ca^{2+} Concentrations in Single Smooth Muscle Cells

John G. McCarron¹, Kurt I. Anderson², Amanda J. Wright¹, John M. Girkin¹

¹ University of Strathclyde, Glasgow, United Kingdom

² University of Glasgow, Glasgow, United Kingdom.

Board B216

In smooth muscle, Ca^{2+} controls diverse activities which include cell division, contraction and cell death. Of particular significance in enabling Ca^{2+} to perform these multiple functions is the cell's ability to localize Ca^{2+} signals to certain regions by creating high local concentrations of Ca^{2+} (microdomains) which differ from the cytoplasmic average. Microdomains are acknowledged to occur near the plasma membrane as a result of Ca^{2+} influx, but measuring them has been difficult. Total internal reflection microscopy (TIRF) enables optical sectioning via the use of evanescent wave illumination. In a TIRF system, fluorescence excitation is restricted to within ~200 nm of the coverslip thus it is possible to selectively image the subplasma membrane space. Here subplasma membrane and bulk cytoplasmic average $[\text{Ca}^{2+}]$ have been measured simultaneously using TIRF and wide field fluorescent imaging in single voltage clamped smooth muscle cells. A single Ca^{2+} indicator (fluo-3) was used to measure both subplasma membrane $[\text{Ca}^{2+}]$ and bulk cytoplasmic average $[\text{Ca}^{2+}]$ to simplify analysis of the results since only one set of kinetic parameters and affinity apply in calibrating the

Ca^{2+} signals. The results show that, in single voltage clamped smooth muscle cells at rest (-70 mV), the $[\text{Ca}^{2+}]$ in the subplasma membrane space was approximately double the bulk cytoplasmic average value. During brief depolarizations to +10 mV the subplasma membrane $[\text{Ca}^{2+}]$ was approximately five times greater than the cytoplasmic average value.

Supported by the Wellcome Trust and British Heart Foundation

Mitochondrial Channels & Calcium Signaling

1241-Pos Harmonic Generation Spectroscopy of Live Cells: Measurements and Volterra Series Analysis

Hans L. Infante, Jie Fang, Kimal Rajapakshe, William R. Widger, John H. Miller

University of Houston, Houston, TX, USA.

Board B217

We report on measurements and analysis of the fundamental (linear response) and higher harmonics (nonlinear responses) generated by suspensions of live cells, including *S. cerevisiae* (budding yeast) and *S. pombe* (fission yeast), in response to sinusoidal electric fields. Their frequency- and time-dependences exhibit features that correlate with consumption of glucose and oxygen, possibly due to oxidative phosphorylation within the mitochondria. These and other biological systems exhibit nonlinear responses that require a more accurate analysis than that afforded by linearization of the model system. For example, Fourier and Laplace transforms only treat the response of the system at the applied fundamental frequency. By contrast, the higher harmonics and other manifestations of nonlinear response can be treated through the application of Volterra theory. The Volterra series representation thus obtained is not only an explicit nonlinear representation of the system's response to the input signal, but also affords greater insight into the biological system's operation. We discuss the application of Volterra theory to the analysis of systems modeled in terms of certain nonlinear differential equations that include damping. Our main objective here is to describe, and qualitatively understand, the observed behavior of the second harmonic vs. time and frequency. We interpret the behavior in terms of parameter changes within a simple mathematical model, and try to correlate those changes with actual biological processes.

1242-Pos Two Commercially-Available Antibodies to Kir6.1 Recognize Non-Target Proteins in Bovine Heart Mitochondria

D. Brian Foster, Jasma Rucker, Eduardo Marban

Johns Hopkins School of Medicine, Baltimore, MD, USA.